Optimal Control of Magnetization Reversal in a Monodomain Particle by Means of Applied Magnetic Field

Grzegorz J. Kwiatkowski,[1] Mohammad H. A. Badarneh,[1] Dmitry V. Berkov,[2] and Pavel F. Bessarab[1,3,4,*]
[1]*Science Institute of the University of Iceland, 107 Reykjavík, Iceland*
[2]*General Numerics Research Lab, Moritz-von-Rohr-Straße 1A, 07745 Jena, Germany*
[3]*ITMO University, 197101 St. Petersburg, Russia*
[4]*Peter Grünberg Institute and Institute for Advanced Simulation, Forschungszentrum Jülich, 52425 Jülich, Germany*

(Received 20 April 2020; accepted 5 April 2021; published 29 April 2021)

A complete analytical solution to the optimal reversal of a macrospin with easy-axis anisotropy is presented. An optimal control path minimizing the energy cost of the reversal is identified and used to derive the time-dependent direction and amplitude of the optimal switching field. The minimum energy cost of the reversal scales inversely with the switching time for fast switching, follows exponential asymptotics for slow switching, and reaches the lower limit proportional to the energy barrier between the target states and to the damping parameter at infinitely long switching time. For a given switching time, the energy cost is never smaller than that for a free macrospin. This limitation can be bypassed by adding a hard anisotropy axis that activates the internal torque in the desired switching direction, thereby significantly reducing the energy cost. A comparison between the calculated optimal control path and minimum energy path reveals that optimal control does not translate to the minimization of the energy barrier but signifies effective use of the system's internal dynamics to aid the desired magnetic transition.

DOI: 10.1103/PhysRevLett.126.177206

Exact results concerning energy-efficient manipulation of magnetic structure are highly important for fundamental science and also for technological applications, as they could help improve the performance of computing and memory devices based on magnetic elements. Optimization of magnetization switching in bistable nanomagnets by tuning the external magnetic field has come under special focus. It has been shown that a switching field can be significantly reduced by application of a weak radio frequency field pulse [1–11]. Magnetization reversal can be achieved exclusively by a microwave field [2], whose amplitude can be reduced provided that the frequency is properly modulated [12–16]. Sun and Wang [17] obtained a theoretical limit of the minimal switching field and derived an optimal constant-amplitude pulse yielding the shortest switching time. Assuming a fixed magnitude but variable direction of the switching field, Wang *et al.* [18] derived the Euler-Lagrange equations for the fastest reversal of an arbitrary Stoner particle. Barros *et al.* [19] developed a general theoretical framework for the design of control field pulses that minimize the energy cost of switching, calculated numerically the optimal switching field for a macrospin with easy-axis anisotropy, and derived analytically the asymptotic properties of the reversal for infinitely long switching time [20]. So far, theoretical studies of optimal magnetization switching have imposed constraints on the switching field or involved numerical simulations, but a general analytical solution providing a transparent physical picture is still missing.

Here we present a complete analytical solution to the problem of energy-efficient switching of a nanomagnet with easy-axis anisotropy. In contrast to previous studies, our solution does not involve any assumptions about the shape of the optimal switching pulse, therefore providing a true theoretical limit to the energy cost of the switching as a function of the switching time and establishing a link between the optimal pulse and material properties. Our results reveal new fundamental properties of the reversal, including two asymptotic regimes of the energy cost and the optimal switching time. The easy-axis anisotropy cannot reduce the energy cost of switching compared with the free-macrospin case, but this limitation can be lifted by introducing a hard anisotropy axis in the system. Energy-efficient magnetization switching in the system with the hard axis illustrates the concept of using the system's internal dynamics to aid the desired change in the magnetic structure, thereby offering a new perspective on the design of magnetic memory elements.

The efficiency of the magnetization reversal is enhanced by minimizing the energy losses associated with the generation of the switching field. Assuming an electric circuit to be the source of the field and neglecting the losses on radiation, the energy cost is defined by Joule heating due to the resistance of the circuit. This is proportional to the electric current square integrated over the switching time. Taking into account the linear relationship between the current magnitude and the strength of the

generated field, we arrive at the cost functional proposed by Barros *et al.* [19]:

$$\Phi = \int_0^T |\vec{b}|^2 dt, \tag{1}$$

where T is the switching time and $\vec{b}$ is the generated time-dependent magnetic field. The functional Φ needs to be minimized subject to boundary conditions and a constraint imposed by the equation of motion for the magnetic moment, chosen here to be the zero-temperature Landau-Lifshitz-Gilbert equation [21]

$$(1+\alpha^2)\dot{\vec{s}} = -\gamma\vec{s}\times(\vec{b}_i+\vec{b}) - \alpha\gamma\vec{s}\times[\vec{s}\times(\vec{b}_i+\vec{b})], \tag{2}$$

where α is the Gilbert damping, γ is the gyromagnetic ratio, and $\vec{s}$ is the unit vector along the magnetic moment $\vec{\mu}$. The internal field is defined as $\vec{b}_i = -\mu^{-1}\partial E/\partial\vec{s}$, with E being the energy of the system excluding the Zeeman term.

The constrained minimization of Φ can be formulated as an unconstrained optimization by expressing $\vec{b}$ in terms of the dynamical trajectory of the system as well as the internal magnetic field,

$$\vec{b} = \frac{\alpha}{\gamma}\dot{\vec{s}} + \frac{1}{\gamma}[\vec{s}\times\dot{\vec{s}}] - \vec{b}_i^{\perp}. \tag{3}$$

Here $\vec{b}_i^{\perp} \equiv \vec{b}_i - (\vec{s}\cdot\vec{b}_i)\vec{s}$, which is the transverse component of $\vec{b}_i$ (the longitudinal component is not included, as it does not affect the dynamics). On substituting (3) into (1), the energy cost of the reversal becomes a functional of the switching trajectory. By solving the Euler-Lagrange equation, the trajectory minimizing the cost functional Φ can be found. We denote this trajectory as the optimal control path (OCP) so as to distinguish it from other switching trajectories and to highlight its physical meaning. The optimal switching pulse can be obtained from the OCP using Eq. (3), thereby derived from the system's intrinsic magnetic properties, which are available via well-established techniques [22]. A similar paradigm was used to optimize electric current driving domain walls in nanowires [23].

We apply the concept outlined above to a uniaxial single-domain particle whose magnetic moment is reversed from one stable orientation to the other (see Fig. 1). The energy barrier between the stable states is assumed to be much larger than the thermal energy. This model mimics, e.g., a bit operation in a nanoscale magnetic memory element, where strong magnetic anisotropy ensures stability of the element against thermal fluctuations [24]. The internal energy E of the system is defined by the anisotropy along the z axis,

$$E = -Ks_z^2, \tag{4}$$

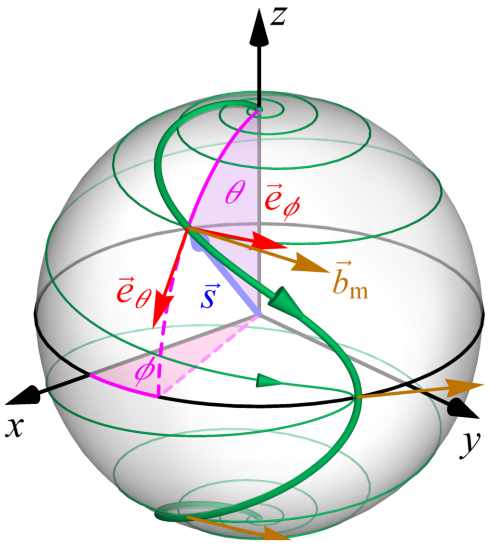

FIG. 1. Calculated optimal control paths (OCPs) for the reversal of a macrospin pointing along the unit vector $\vec{s}$. The initial and the final states are at the north and the south poles of the unit sphere, respectively. The damping factor α is 0.1. The switching time T is $10\tau_0$ and $100\tau_0$ for the paths shown with thick and thin green lines, respectively. The external magnetic field $\vec{b}_m$ at $t = T/4$, $t = T/2$, and $t = 3T/4$ is shown for the shorter path with the brown arrows.

where $K > 0$ is the anisotropy constant. Euler-Lagrange equations in spherical coordinates θ and ϕ (Fig. 1) read

$$\tau_0^2\ddot{\theta} = \frac{\alpha^2}{4(1+\alpha^2)^2}\sin 4\theta, \qquad \tau_0\dot{\phi} = \frac{\cos\theta}{1+\alpha^2}, \tag{5}$$

where the period of Larmor precession $\tau_0 = \mu(2\gamma K)^{-1}$ defines the timescale. The boundary conditions $\theta(0) = 0$, $\theta(T) = \pi$ correspond to the transition between the energy minima within the switching time T. Equation (5) for θ is the well-known Sine-Gordon equation [25,26], whose solutions are expressed by Jacobi elliptic functions [27,31]. The OCP described by Eq. (5) reveals the mechanism for the reversal: The moment moves steadily from the initial state upward the energy surface while precessing counterclockwise around the anisotropy axis until it reaches the top of the energy barrier at $t = T/2$. At this point, the precession reverses its direction and the system slides down to the target state minimum. This scenario was obtained numerically by Barros *et al.* [19,20], but the exact analytical solution makes it possible to derive general properties of the OCP [27].

Substitution of the solution for θ and ϕ into Eq. (3) results in the following expressions for the optimal switching field:

$$\vec{b}_m = \frac{b_m}{\sqrt{1+\alpha^2}}(\alpha\vec{e}_\theta + \vec{e}_\phi), \tag{6}$$

$$b_m = \frac{K}{\mu p\sqrt{1+\alpha^2}}\left[\mathrm{dn}\left(\frac{t}{p\tau_0(1+\alpha^2)}\middle| -\alpha^2 p^2\right) + \alpha p\,\mathrm{sn}\left(\frac{t}{p\tau_0(1+\alpha^2)}\middle| -\alpha^2 p^2\right)\right], \tag{7}$$

where $\vec{e}_\theta$, $\vec{e}_\phi$ are local time-dependent orthonormal vectors in the directions of increasing θ, and ϕ, respectively (see Fig. 1), while dn(.|.) and sn(.|.) are Jacobi elliptic functions [27,31] and p is a parameter implicitly defined through the following equation: $T = 4\tau_0(1+\alpha^2)p\mathcal{K}(-\alpha^2 p^2)$, with $\mathcal{K}(.)$ being the complete elliptic integral of the first kind [27,31]. Equation (6) signifies that the switching field points in a specific fixed direction in the time-varying frame of reference associated with the magnetic moment [17] evolving according to Eq. (5). The orientation of the field is such that its contribution to the precession around the anisotropy axis is exactly zero, and the external pulse contributes only to the part of motion that is relevant for switching, i.e., progressive increase in θ. The optimal orientation of the switching field can be obtained regardless of optimization of the pulse amplitude; e.g., Eq. (6) still holds for the constant field amplitude [17].

Equation (7) describes the optimal switching field amplitude b_m (see Fig. 2). When $\alpha = 0$, the amplitude is time independent: $b_m|_{\alpha=0} = \pi/(\gamma T)$. Note that for zero α there is no energy consumption by the magnetic moment itself, but energy is still expended on the creation of the switching field. We emphasize that the functional Φ characterizes the energy spent by the external field source and not the energy dissipated in the magnetic system.

For $\alpha > 0$, $b_m(t)$ has a more complex structure, but the symmetry $b_m(0) = b_m(T/2) = b_m(T)$ holds. Damping gives rise to the internal torque in the polar direction. This torque—produced by the anisotropy field—counteracts the switching motion before crossing the equator, and a maximum in the switching field forms at $t = T/4$ so as to neutralize this effect (see Fig. 2). After the trajectory has crossed the equator at $t = T/2$ [27], the internal torque aids the switching, and b_m reaches a minimum at $t = 3T/4$. The position of the maximum and the minimum of $b_m(t)$ coincides with that of the extrema of the polar component of the internal torque (see Fig. 2). Note that the external field, although reduced compared to that before barrier crossing, is still nonzero in general: Some field needs to be applied in order to terminate the reversal on time. However, for long enough switching time, $T \gg (\alpha + 1/\alpha)\tau_0$, damping alone is sufficient to complete the switching, and virtually no field needs to be applied after crossing the energy barrier (see black curve in Fig. 2). Although the magnitude of neither maximum $b_{\max}$ nor minimum $b_{\min}$ of the switching field amplitude can be described in terms of elementary functions in a general case, the difference between them is always

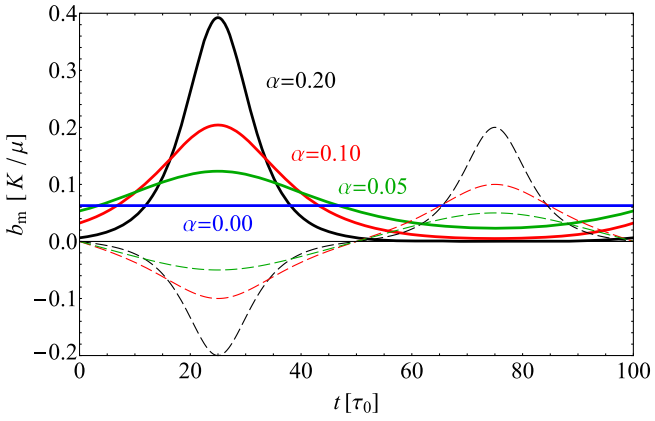

FIG. 2. Amplitude of the switching field as a function of time for $T = 100\tau_0$ and several values of α (solid lines). Dashed lines show $\alpha b_i^{\perp}$, which is proportional to the polar component of the torque generated by the internal field.

$$\Delta b = b_{\max} - b_{\min} = \frac{2\alpha K}{\mu\sqrt{1+\alpha^2}}. \tag{8}$$

Moreover, the average amplitude b_{av} can be computed analytically, leading to an exact relation

$$b_{\mathrm{av}} = \frac{1}{T}\int_0^T b_m(t)dt = \frac{\pi\sqrt{1+\alpha^2}}{\gamma T}, \tag{9}$$

which demonstrates that overall larger fields are required to terminate the reversal in a shorter time, as expected. Interestingly, b_{av} does not depend on the magnetic potential. From Eqs. (8) and (9) it follows that $\Delta b/b_{\mathrm{av}} \to 0$ for $T \to 0$; i.e., a decrease in the switching time progressively makes $b_m(t)$ resemble a time-independent function [27].

Equation (7) recovers the result of Barros *et al.* for $T \to \infty$—see Eq. (13) in Ref. [20]—as well as that of Sun and Wang for $\alpha = 0$—see Eqs. (7) and (9) in Ref. [17]. Additionally, for $T \ll (\alpha + 1/\alpha)\tau_0$ the pulse amplitude simplifies to $b_m \approx b_{\mathrm{av}} + \Delta b \sin(2\pi t/T)/2$.

Substitution of Eq. (7) into Eq. (1) leads to the following formula for the minimum energy cost:

$$\Phi_m = \frac{2K[2\mathcal{E}(-\alpha^2 p^2) - \mathcal{K}(-\alpha^2 p^2)]}{\gamma\mu p}, \tag{10}$$

where $\mathcal{E}(.)$ is the complete elliptic integral of the second kind [27,31]. According to (10), Φ_m is a monotonically decreasing (increasing) function of the switching time T (damping parameter α), as illustrated in Fig. 3. Energy cost as a function of the switching time has two asymptotic regimes corresponding to fast and slow switching. For the short switching time, the magnetic potential becomes irrelevant, and $\Phi_m(T)$ is described by a power law:

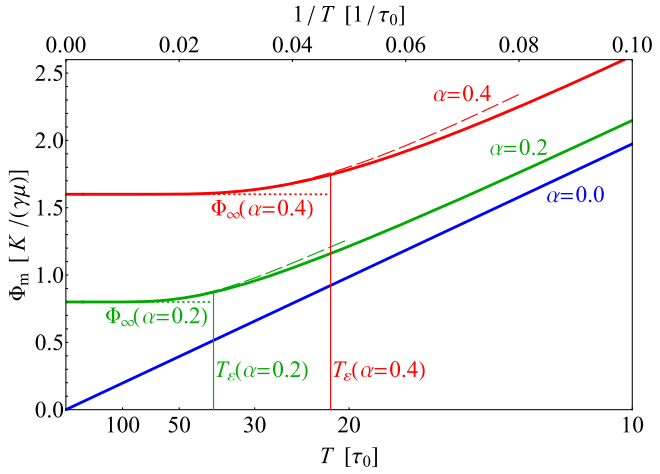

FIG. 3. Minimum energy cost of magnetization switching as a function of the inverse of the switching time. Dashed (dotted) lines show long (infinite) switching time asymptotics. Thin vertical lines indicate switching time T_ε, for which the minimum energy cost is $\varepsilon = 10\%$ larger than the infinite switching time limit Φ_∞.

$$\Phi_m \approx \frac{\pi^2(1+\alpha^2)}{\gamma^2 T} + O(T), \quad T \ll (\alpha + 1/\alpha)\tau_0, \tag{11}$$

The leading term in Eq. (11) specifically recovers the potential-free case. The power-law regime changes to an exponential dependence on T for the long switching time:

$$\Phi_m \approx \Phi_\infty \left(1 + 4\exp\left[-\frac{\alpha T}{2\tau_0(1+\alpha^2)}\right]\right), \quad T \gg (\alpha + 1/\alpha)\tau_0, \tag{12}$$

which particularly demonstrates that, for a given anisotropy constant and damping parameter, the lower limit of the energy cost is $\Phi_\infty \equiv 4\alpha K/(\gamma\mu)^{-1}$, as predicted in [20]. Strictly speaking, this limit is reached at infinitely long switching time, but Eq. (12) makes it possible to analyze to what extent the limit can be approached within finite T. In particular, termination of the reversal within time $T_\varepsilon = 2\ln(4/\varepsilon)[\alpha + 1/\alpha]\tau_0$ corresponds to the energy cost that is only by a fraction of $\varepsilon < 1$ larger than Φ_∞: $\Phi_m(T_\varepsilon)/\Phi_\infty = 1 + \varepsilon$. Therefore, T_ε has a meaning of optimal switching time in a sense that increase in T beyond T_ε does not lead to a significant gain in energy efficiency (see Fig. 3).

Analysis of Eq. (10) shows that for a given switching time T, the energy cost is never smaller than that in a zero-potential case: $\Phi_m(T) \geq \Phi_0(T) \equiv \pi^2(1+\alpha^2)/(\gamma^2 T)$, where the equality is reached for $\alpha = 0$. In other words, the internal energy obstructs the reversal in a system with easy-axis anisotropy, and the purpose of the pulse optimization in this case is to minimize the unfavorable effect caused by the magnetic potential. To be able to use the internal energy landscape to aid the switching process, additional terms in the magnetic potential are necessary. We have found that the energy cost can be reduced by adding a hard-axis anisotropy to the system. The internal energy $\tilde{E}$ of such a biaxial anisotropy system can be written as

$$\tilde{E} = -K s_y^2 + K_h s_z^2, \tag{13}$$

where the easy axis and the hard axis are along the y and z directions, respectively. The hard-axis anisotropy constant K_h is taken to be 10 times larger than K. This $K_h \gg K$ regime can be realized thanks to the large demagnetizing field [32] in thin flat elongated nanoelements. Such structures are used, e.g., as single bits in in-plane memory designs [24], or as elements of artificial spin ice systems [33,34]. The OCP between the energy minima at $s_y = \pm 1$ was obtained by a direct numerical minimization of the energy cost functional for the switching time $T = 0.32\tau_0$ and damping $\alpha = 0$. Surprisingly, the corresponding energy cost $\tilde{\Phi}_m$ turned out to be an order of magnitude smaller than that for the reversal with the same switching time and damping in the system with zero magnetic potential: $\tilde{\Phi}_m/\Phi_0 \approx 0.088$. This phenomenon can be explained by the distribution of the internal torque; see Fig. 4. Because of the hard axis, there is a region in the configuration space where the system's internal torque systematically points in the desired switching direction. By placing the switching path into this region, the optimal control efficiently exploits the internal torque to assist the switching. The external pulse has a minimal influence; its purpose is only to trigger the switching by directing the system toward the particular sector in the configuration space where the internal dynamics picks the system up and drags it to the desired target state. This effect was also noticed earlier for in-plane magnetized Co films [35] and Co nanoclusters characterized by complex magnetic anisotropy [36].

Finally, we compare our OCP with another distinguished path in the configuration space—the minimum energy path (MEP). An MEP connecting two stable states is a path lying lowermost on the energy surface, and the point of highest energy along the MEP defines the energy barrier within harmonic rate theories [37–39]. The MEP for the magnetization reversal in the biaxial system is the shortest path connecting the energy minima through the saddle point at $\theta = \pi/2$, $\phi = \pi$ (see Fig. 4). This path is very different from the calculated OCP, which demonstrates a more complex structure. To emphazise the difference between MEP and OCP, we note that the OCP is a dynamical trajectory defined by the parameters of the equation of motion, whereas the MEP is determined entirely by the energy surface of the system. Since the OCP does not even pass through the saddle point, the energy maximum along the OCP is higher than the energy barrier derived from the MEP (see the inset in Fig. 4). This result means that optimal

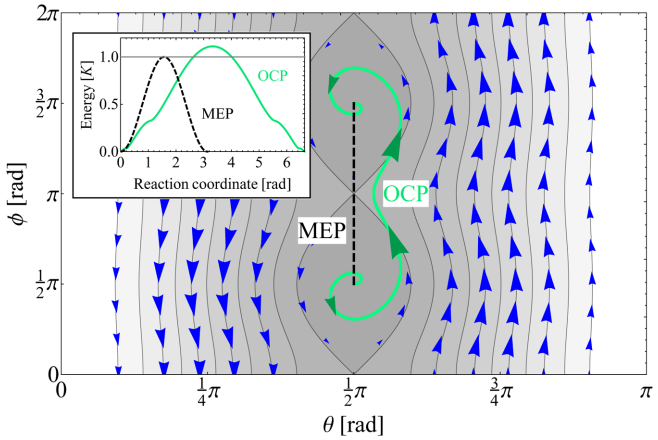

FIG. 4. Distribution of the torque (blue arrows) generated by the internal field of the macrospin system with both easy and hard anisotropy axes, superimposed on the contour plot showing the energy surface of the system defined by Eq. (13). The green line shows the calculated OCP for $T = 0.32\tau_0$ and $\alpha = 0$. Green arrows indicate the velocity of the system. The size of the blue (green) arrows code the magnitude of the torque (velocity). The black dashed line shows the minimum energy path (MEP). The inset shows the energy of the system as a function of displacement along the OCP (green solid line) and MEP (black dashed line).

control of a magnetic transition does not necessarily lead to a path that minimizes the energy barrier between the target states. Following an OCP involves rotation of magnetic moments in such a way that the influence of the external stimulus is minimized, but the system's internal dynamics is effectively used to aid the magnetic transition.

Experimental realization of optimal control pulses, such as the one given by Eqs. (6) and (7), is challenging but still feasible within current technology for pulse shaping [40–45]. Note also that the optimal switching protocol derived here is quite stable with respect to thermal fluctuations and material parameter perturbations, as confirmed by our spin dynamics simulations [27].

In conclusion, we have presented an exact analytical solution to the problem of optimal switching of a nanomagnet via the coherent magnetization rotation mode used in most modern magnetic memories. The easy-axis anisotropy alone can only increase the energy cost of the switching compared to the free-macrospin case, but this effect is minimized by following the OCP. The system's internal torque can be used to aid the switching by introducing a hard anisotropy axis. Our results deepen the understanding of the optimal control of magnetization switching in nanoparticles and provide guiding principles for the design of energy-efficient digital devices based on magnetic elements.

The authors would like to thank H. Jónsson, B. Hjörvarsson, V. Kapaklis, and T. Sigurjónsdóttir for helpful discussions. This work was funded by the Russian Science Foundation (Grant No. 19-72-10138), the Icelandic Research Fund (Grant No. 184949-052), the Deutsche Forschungsgemeinschaft (DFG Grant No. BE2464/17-1), and the Alexander von Humboldt Foundation.

*bessarab@hi.is

[1] C. Thirion, W. Wernsdorfer, and D. Mailly, Switching of magnetization by nonlinear resonance studied in single nanoparticles, Nat. Mater. **2**, 524 (2003).
[2] Z. Z. Sun and X. R. Wang, Magnetization reversal through synchronization with a microwave, Phys. Rev. B **74**, 132401 (2006).
[3] G. Woltersdorf and C. H. Back, Microwave assisted switching of single domain $Ni_{80}Fe_{20}$ elements, Phys. Rev. Lett. **99**, 227207 (2007).
[4] J.-G. Zhu, X. Zhu, and Y. Tang, Microwave assisted magnetic recording, IEEE Trans. Magn. **44**, 125 (2008).
[5] S. Okamoto, N. Kikuchi, and O. Kitakami, Magnetization switching behavior with microwave assistance, Appl. Phys. Lett. **93**, 102506 (2008).
[6] S. Okamoto, N. Kikuchi, and O. Kitakami, Frequency modulation effect on microwave assisted magnetization switching, Appl. Phys. Lett. **93**, 142501 (2008).
[7] G. Bertotti, I. D. Mayergoyz, C. Serpico, M. d'Aquino, and R. Bonin, Nonlinear-dynamical-system approach to microwave-assisted magnetization dynamics (invited), J. Appl. Phys. **105**, 07B712 (2009).
[8] Z. Wang and M. Wu, Chirped-microwave assisted magnetization reversal, J. Appl. Phys. **105**, 093903 (2009).
[9] R. Yanes, R. Rozada, F. García-Sánchez, O. Chubykalo-Fesenko, P. M. Pimentel, B. Leven, and B. Hillebrands, Modeling of microwave-assisted switching in micron-sized magnetic ellipsoids, Phys. Rev. B **79**, 224427 (2009).
[10] S. Okamoto, N. Kikuchi, M. Furuta, O. Kitakami, and T. Shimatsu, Switching Behaviors and its Dynamics of a Co/Pt Nanodot under the Assistance of rf Fields, Phys. Rev. Lett. **109**, 237209 (2012).
[11] S. Okamoto, M. Furuta, N. Kikuchi, O. Kitakami, and T. Shimatsu, Theory and experiment of microwave-assisted magnetization switching in perpendicular magnetic nanodots, IEEE Trans. Magn. **50**, 83 (2014).
[12] K. Rivkin and J. B. Ketterson, Magnetization reversal in the anisotropy-dominated regime using time-dependent magnetic fields, Appl. Phys. Lett. **89**, 252507 (2006).
[13] Z. Z. Sun and X. R. Wang, Strategy to reduce minimal magnetization switching field for Stoner particles, Phys. Rev. B **73**, 092416 (2006).
[14] L. Cai, D. A. Garanin, and E. M. Chudnovsky, Reversal of magnetization of a single-domain magnetic particle by the ac field of time-dependent frequency, Phys. Rev. B **87**, 024418 (2013).
[15] G. Klughertz, P.-A. Hervieux, and G. Manfredi, Autoresonant control of the magnetization switching in single-domain nanoparticles, J. Phys. D **47**, 345004 (2014).
[16] M. T. Islam, X. S. Wang, Y. Zhang, and X. R. Wang, Subnanosecond magnetization reversal of a magnetic nanoparticle driven by a chirp microwave field pulse, Phys. Rev. B **97**, 224412 (2018).

[17] Z. Z. Sun and X. R. Wang, Theoretical limit of the minimal magnetization switching field and the optimal field pulse for Stoner particles, Phys. Rev. Lett. **97**, 077205 (2006).

[18] X. R. Wang, P. Yan, J. Lu, and C. He, Euler equation of the optimal trajectory for the fastest magnetization reversal of nano-magnetic structures, Europhys. Lett. **84**, 27008 (2008).

[19] N. Barros, M. Rassam, H. Jirari, and H. Kachkachi, Optimal switching of a nanomagnet assisted by microwaves, Phys. Rev. B **83**, 144418 (2011).

[20] N. Barros, H. Rassam, and H. Kachkachi, Microwave-assisted switching of a nanomagnet: Analytical determination of the optimal microwave field, Phys. Rev. B **88**, 014421 (2013).

[21] D. V. Berkov, Magnetization dynamics including thermal fluctuations: Basic phenomenology, fast remagnetization processes and transitions over high-energy barriers, in *Handbook of Magnetism and Advanced Magnetic Materials*, edited by H. Kronmüller and S. Parkin (John Wiley & Sons, Chichester, UK, 2007), Vol. 2, pp. 795–823.

[22] A. Barman and J. Sinha, *Spin Dynamics and Damping in Ferromagnetic Thin Films and Nanostructures* (Springer, Cham, Switzerland, 2018).

[23] O. A. Tretiakov, Y. Liu, and A. Abanov, Minimization of Ohmic Losses for Domain Wall Motion in a Ferromagnetic Nanowire, Phys. Rev. Lett. **105**, 217203 (2010).

[24] K. C. Chun, H. Zhao, J. D. Harms, T.-H. Kim, J.-P. Wang, and C. H. Kim, A scaling roadmap and performance evaluation of in-plane and perpendicular MTJ based STT-MRAMs for high-density cache memory, IEEE J. Solid-State Circuits **48**, 598 (2013).

[25] H. Mikeska, Solitons in a one-dimensional magnet with an easy plane, J. Phys. C **11**, L29 (1978).

[26] J. Cuevas-Maraver, P. G. Kevrekidis, and F. Williams, *The Sine-Gordon Model and its Applications* (Springer, Cham, Switzerland, 2014).

[27] See Supplemental Material at http://link.aps.org/supplemental/10.1103/PhysRevLett.126.177206 for the definitions of elliptic functions and integrals, discussion of the OCP and its symmetries, results of spin dynamics simulations showing stability of the optimal switching protocol against thermal fluctuations and material parameter perturbations, a figure showing the OCP as a function of time and α, a figure showing $b_{\min}$, $b_{\max}$, b_{av} as functions of α and T, and a figure illustrating how $b_m(t)$ profile changes with T, which includes Refs. [28–30].

[28] J. H. Mentink, M. V. Tretyakov, A. Fasolino, M. I. Katsnelson, and T. Rasing, Stable and fast semi-implicit integration of the stochastic Landau–Lifshitz equation, J. Phys. Condens. Matter **22**, 176001 (2010).

[29] H. Richter, Density limits imposed by the microstructure of magnetic recording media, J. Magn. Magn. Mater. **321**, 467 (2009).

[30] M. Krounbi, V. Nikitin, D. Apalkov, J. Lee, X. Tang, R. Beach, D. Erickson, and E. Chen, Status and challenges in spin-transfer torque MRAM technology, ECS Trans. **69**, 119 (2015).

[31] *Handbook of Mathematical Functions with Formulas, Graphs, and Mathematical Tables*, edited by M. Abramowitz and I. A. Stegun (National Bureau of Standards, Washington, DC, 1964).

[32] J. A. Osborn, Demagnetizing factors of the general ellipsoid, Phys. Rev. **67**, 351 (1945).

[33] C. Nisoli, R. Moessner, and P. Schiffer, Colloquium: Artificial spin ice: Designing and imaging magnetic frustration, Rev. Mod. Phys. **85**, 1473 (2013).

[34] G. M. Wysin, W. A. Moura-Melo, L. A. S. Mól, and A. R. Pereira, Magnetic anisotropy of elongated thin ferromagnetic nanoislands for artificial spin ice arrays, J. Phys. Condens. Matter **24**, 296001 (2012).

[35] C. H. Back *et al.*, Minimum field strength in precessional magnetization reversal, Science **285**, 864 (1999).

[36] C. Etz, M. Costa, O. Eriksson, and A. Bergman, Accelerating the switching of magnetic nanoclusters by anisotropy-driven magnetization dynamics, Phys. Rev. B **86**, 224401 (2012).

[37] H. Kramers, Brownian motion in a field of force and the diffusion model of chemical reactions, Physica (Amsterdam) **7**, 284 (1940).

[38] G. H. Vineyard, Frequency factors and isotope effects in solid state rate processes, J. Phys. Chem. Solids **3**, 121 (1957).

[39] W. F. Brown, Thermal fluctuation of fine ferromagnetic particles, IEEE Trans. Magn. **15**, 1196 (1979).

[40] T. Gerrits, H. A. M. van den Berg, J. Hohlfeld, L. Bär, and T. Rasing, Ultrafast precessional magnetization reversal by picosecond magnetic field pulse shaping, Nature (London) **418**, 509 (2002).

[41] T. P. M. Alegre, A. C. Torrezan, and G. Medeiros-Ribeiro, Microstrip resonator for microwaves with controllable polarization, Appl. Phys. Lett. **91**, 204103 (2007).

[42] M. Curcic *et al.*, Polarization Selective Magnetic Vortex Dynamics and Core Reversal in Rotating Magnetic Fields, Phys. Rev. Lett. **101**, 197204 (2008).

[43] H. Gao, C. Lei, M. Chen, F. Xing, H. Chen, and S. Xie, A simple photonic generation of linearly chirped microwave pulse with large time-bandwidth product and high compression ratio, Opt. Express **21**, 23107 (2013).

[44] A. Bisig *et al.*, Dynamic domain wall chirality rectification by rotating magnetic fields, Appl. Phys. Lett. **106**, 122401 (2015).

[45] M. Rius, M. Bolea, J. Mora, and J. Capmany, Incoherent photonic processing for chirped microwave pulse generation, IEEE Photonics Technol. Lett. **29**, 7 (2017).